J. Cosmet. Sci., 54, 589–598 (November/December 2003)

Bioconvertible vitamin antioxidants improve sunscreen photoprotection against UV-induced reactive oxygen species

KERRY M. HANSON and ROBERT M. CLEGG, *Laboratory for Fluorescence Dynamics, Department of Physics, University of Illinois, Urbana-Champaign, Illinois.*

Accepted for publication May 20, 2003.

Synopsis

The ability of sunscreens and antioxidants to deactivate highly destructive reactive oxygen species in human skin has remained inconclusive. Two-photon fluorescence imaging microscopy was used to determine the effect of sunscreen/antioxidant combinations upon UV-induced ROS generation in *ex vivo* human skin. A sunscreen combination containing octylmethoxycinnamate (Parsol® MCX) and avobenzone (Parsol® 1789) at SPF 8 and SPF 15 was tested for its ability to prevent UV radiation from generating ROS in the viable epidermal strata of *ex vivo* human skin. A UV dose equivalent to two hours of North American solar UV was used to irradiate the skin. Each sunscreen reduced the amount of ROS induced in the viable strata by a value consistent with the SPF level. UV photons that were not absorbed/scattered by the sunscreen formulations generated ROS within the viable epidermal layers.

The addition of the bioconvertible antioxidants vitamin E acetate and sodium ascorbyl phosphate (STAY-C® 50) improves photoprotection by converting to vitamins E and C, respectively, within the skin. The bioconversion forms an antioxidant reservoir that deactivates the ROS generated (within the strata granulosum, spinosum, and basale) by the UV photons that the sunscreens do not block in the stratum corneum.

INTRODUCTION

Ultraviolet (UV) irradiation of human skin induces the generation of reactive oxygen species (ROS), including singlet oxygen ($^1O_2$), hydrogen peroxide (H_2O_2), and/or peroxynitrite ($ONOO^-$) (1). These highly reactive derivatives of molecular oxygen react with cellular components including lipid membranes and are considered a source of photoaging and skin cancers that appear later in life (2–9). The ability of sunscreens to protect against the generation of ROS within the skin has not been identified. Although sunscreens do prevent erythema, and are recommended to be used as part of safe-sun practices (10), current research suggests that photoprotection is also needed to reduce ROS levels within the skin (11,12).

Address all correspondence to Kerry M. Hanson.

Antioxidants have recently been added to formulations to deactivate ROS levels (12); however, similar to our limited understanding of sunscreen-mediated ROS photoprotection, whether or not the addition of antioxidants enhances photoprotection against UV-induced ROS generation is not well understood. This can be attributed predominantly to limitations in technology that, until recently, have not allowed for the study of cellular processes within the opaque and heterogeneous environment of the skin. Clearly, understanding the effect of sunscreens and antioxidants upon the level of UV-induced ROS generated under biologically relevant conditions (i.e., in viable human skin, at a commonly obtained UV dose) will aid our understanding of the efficacy of these formulations and lead to improved photoprotection.

We have recently developed a two-photon fluorescence microscopy method with submicron spatial resolution and submillimeter depth penetration in live human *ex vivo* skin to determine UV-induced ROS levels (1). Following UV irradiation, at a dose equivalent to two hours of North American summer solar UV (1600 J m^{-2}), of human breast tissue, *ca.* 10^{-4} moles of $^1O_2$, H_2O_2 and/or $ONOO^-$ were generated within each epidermal stratum (1). As discussed herein, two-photon fluorescence microscopy serves as an excellent tool to determine the photoprotective effects of sunscreens and antioxidants upon ROS levels generated in epidermis irradiated by a commonly obtained UV dose (1600 J m^{-2}).

MATERIALS AND METHODS

MATERIALS

Reagents. N,N′-[[3′,6′-bis(acetyloxy)-3-oxospiro[isobenzofuran-1(3H),9′-[9H]xanthene]-2′,7′-diyl]bis(methylene)]-bis,N-[2-[(acetyloxy)methoxy]-2-oxoethyl]]-bis[(acetyloxy)-methyl] (calcein-AM), dihydrorhodamine-123 (DHR) and fluorescein diphosphate (FDP) were obtained from Molecular Probes. Sunscreen/antioxidant combinations were provided by Roche Vitamins Inc. Table I lists the active ingredients studied. Two sunscreen formulations with different sun protection factors (SPF) were tested. All ingredients are listed by %-weight. The SPF 8 sunscreen contained 4% octylmethoxycinnamate (OMC, Parsol® MCX) and 2% avobenzone (Parsol® 1789). The SPF 15 sunscreen contained 7.5% OMC and 3% Parsol 1789. Vitamin E acetate and sodium ascorbyl phosphate were added to the formulations at 2.5%.

Skin samples. Ex vivo human skin (breast and facial) was obtained following patient-requested surgery. Samples were obtained with approval from the University of Illinois Internal Review Board. Skin from two individuals was studied. Both skin samples were

Table I
Active Ingredients Listed by %-Weight

Ingredient	SPF 8			SPF 15		
	−E/C	+E	+E/C	−E/C	+E	+E/C
Octylmethoxycinnamate (Parsol® MCX)	4	4	4	7.5	7.5	7.5
Avobenzone (Parsol® 1789)	2	2	2	3	3	3
Vitamin E acetate	0	2.5	2.5	0	2.5	2.5
Sodium ascorbyl phosphate (STAY-C® 50)	0	0	2.5	0	0	2.5

lightly pigmented, although, because of their *ex vivo* nature, their types were not classified. Sample 1 was obtained from the breast of one individual; sample 2 was facial skin from a different individual. Age and gender are not specified due to the requirements of the University of Illinois Internal Review Board. Samples were acquired immediately post-surgery and stored at 4°C in indicator-free RPMI media (Life Technologies) supplemented with gentamicin and L-glutamine until use.

Photoirradiation equipment. UV irradiation of each skin sample was achieved using two UV fluorescence bulbs (T120W/12RS, Philips). The lamp source peaked near 310 nm in the UVB before tapering into the UVA, where <20% of the photons came between 320 nm and 400 nm. Thus, the data acquired are predominately due to UVB-induced reactions. UV irradiance is determined using an energy meter (Model 1825-C, Newport). A total irradiance of 1600 J m^{-2} was selected for two reasons. First, the amount of DHR is not fully converted to rhodamine-123 at this irradiance, which indicates that the amount of DHR present is sufficient to react with the quantity of ROS by a dose of 1600 J m^{-2} (1). Second, an irradiance of 1600 J m^{-2} is a biologically significant UV dose and can be obtained from two hours of noonday summer solar UV exposure in the northern hemisphere (13).

TWO-PHOTON FLUORESCENCE IMAGING MICROSCOPY AND ROS DETECTION IN SKIN

Two-photon excitation is achieved when a molecule simultaneously absorbs two photons at the excitation wavelength. Typically, two-photon excitation is achieved using an ultrafast, pulsed, near-IR laser system (785 nm, 10^{-15} s, titanium:sapphire). Many are familiar with confocal microscopy, which is commercially available. However, compared to UV or visible confocal one-photon sources, two-photon excitation is advantageous for sectioned imaging of the skin, providing reduced photobleaching of the probe fluorophore and limited photodamage to the sample. In addition, Masters *et al.* found that the absence of a pinhole in two-photon excitation allows for greater depth penetration into skin compared to UV confocal excitation (14). As a result, two-photon excitation provides submicron spatial resolution with submillimeter depth penetration such that data can be acquired within the cells of each epidermal stratum and through to the upper dermal layers. In two-photon fluorescence intensity imaging microscopy, the sample is incubated with a fluorophore that can be excited at the two-photon excitation wavelength. Fluorescence probes for a number of chemical reactions or properties within biological samples are available, including those for ROS detection and pH within skin, where a change in fluorescence intensity or lifetime relative to a control sample yields information on the sample (1,15,16).

For example, to study ROS photoprotection within human skin, a five-step procedure is followed to determine the effect of a topical formulation, like a sunscreen- or antioxidant-containing crème, upon UV-induced ROS levels within *ex vivo* skin samples. First, approximately 2 mg cm^{-2} of the formulation is applied to the surface of a skin sample (~0.5 cm × 0.5 cm) and incubated for three hours at 4°C to maintain tissue viability. Second, the sample is incubated for ten minutes at room temperature in a solution containing the ROS-detecting probe dihydrorhodamine (DHR, 100 μM in 2:1 PBS/EtOH). DHR is nonfluorescent until it reacts with $^1O_2$, H_2O_2, and/or $ONOO^-$ (and potentially other ROS), forming fluorescent rhodamine-123 (R123, emission maximum 525 nm) (Figure 1A). Third, the sample is imaged to obtain background (before UV) fluorescence levels for each epidermal stratum. Image areas are between 625 μm^2 and

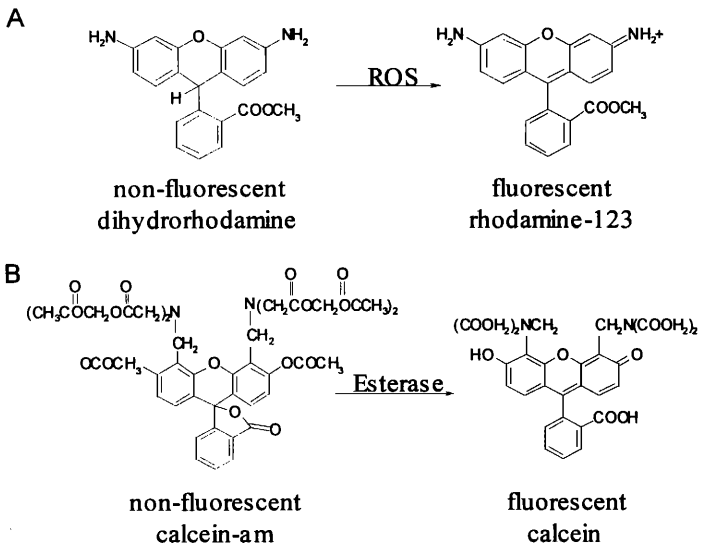

Figure 1. Molecular probes used to detect ROS (A) and esterase activity (B).

4000 μm^2 and are acquired *ca.* every 10 μm, beginning at the stratum corneum surface. Images in the z-direction as little as 2 μm apart can be acquired if desired. Fourth, the skin sample is irradiated by UV (T120W/12RS, Philips), and finally re-imaged. Each image acquired is composed of 256 × 256 pixels. A discussion of the UV source and its differences relative to solar UV radiation is out of the scope of this paper; the reader is referred to other work (1).

In our experiments two-photon excitation is achieved by a Nd:YVO_4 pumped (Millenia, Spectra-Physics) titanium:sapphire laser (Tsunami, Spectra-Physics), whose fundamental at 785 nm is coupled through the epifluorescence port of a Zeiss Axiovert microscope. Fluorescence from the samples is collected by a photomultiplier tube (R3996, Hamamatsu).

IMAGE ANALYSIS

To determine the reduction in UV-induced ROS at depth z due to a test formulation, equation 1 is used:

$$\%-\text{Reduction}(z) = 100 - 100\left(\frac{I(z)_{sample}}{I(z)_{control}}\right) \quad (1)$$

At each epidermal depth z, the fluorescence intensity is calculated over the entire image. These intensity data are averaged together for each skin area studied ($I(z)_{sample}$). At least two unique areas are imaged per skin sample. $I(z)_{control}$ is calculated identically for each area, where the control images are those acquired on skin incubated with DHR only and indicate the control level of ROS that is generated at the UV irradiance used (1600 J m^{-2}). The average reduction in ROS (% reduction_{avg}) is calculated by averaging all % reduction(z) values calculated from each tissue sample.

ESTERASE AND PHOSPHATASE ACTIVITY

To facilitate penetration of the enzymatic activity dyes, the stratum corneum of each skin sample (~0.5 cm × 0.5 m) was removed by tape stripping (Scotch clear tape). These were the only samples in which the stratum corneum was removed. Without removal of the stratum corneum, the enzymatic-activity dyes did not penetrate and enzymatic activity could not be detected. Each sample was incubated at room temperature in a 50-μM calcein-am or fluorescein diphosphate solution (2:1 PBS:EtOH) for ten minutes. Calcein-am is nonfluorescent until active esterases act upon it to form fluorescent calcein (Figure 1B, emission maximum 520 nm). Similarly, fluorescein diphosphate is nonfluorescent until phosphatase activity leads to the formation of fluorescent fluorescein (emission maximum 514 nm). The samples were imaged on the two-photon microscope. Data from two control samples were also acquired on the two-photon microscope: the autofluorescence of the skin sample was collected and the fluorescence intensity of the calcein-am and FDP solutions used for incubation was also collected. The data were used for comparison with the images of skin incubated with dye to determine if enzymatic activity took place.

RESULTS AND DISCUSSION

Because their photoreactions may have a dramatic impact upon photoaging and photocarcinogenesis, we focus upon ROS generation in the keratinocytes of the strata granulosum, spinosum, and basale.

Following irradiation by 1600 J m^{-2} UV of the *ex vivo* breast tissue tested, a dramatic increase in rhodamine-123 fluorescence, and thus ROS levels, was detected in all viable epidermal strata (Figure 2A–C) and in the collagen-rich dermis (Figure 2D). The images indicate the fluorescence intensity expected in the different strata following a UV dose of 1600 J m^{-2}; they represent our controls for the two skin samples. As the images show, ROS are generated predominantly in the cytoplasm of the keratinocytes. This can be seen by noting the red and yellow areas surrounding the blue nuclei. The blue colors indicate the absence of detectable ROS. Because our ROS probe may not have penetrated the nuclear membrane, we cannot comment upon nuclear ROS generation at this time. These images are consistent with previous data (1) and result from the presence of UV-absorbing chromophores present in the cytoplasm of the cells (NADH/NADPH,

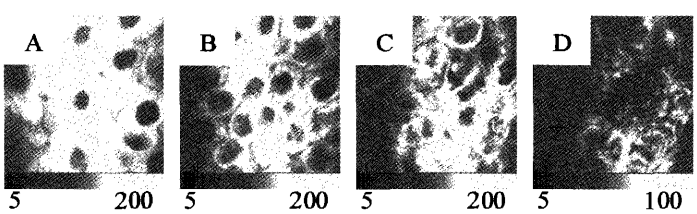

Figure 2. Two-photon fluorescence intensity images of R123 emission in viable *ex vivo* human breast skin following irradiation by 1600 J m^{-2} UV. These images represent the control data used to calculate the effect of the formulations tested upon ROS levels. The corresponding intensity scale bar is displayed below each image, where red represents the maximum number of ROS generated following irradiation. Blue indicates the absence of ROS. Images are displayed of the strata granulosum (A), spinosum (B), basale epidermis (C), and dermis (D). Each image is 50 μm × 50 μm.

riboflavin, tryptophan). Identical results were found for the *ex vivo* facial skin (data not shown).

The photoprotective effects of sunscreens and antioxidants are determined by comparing identically acquired images of the control data against images of skin to which the test formulations were topically applied. As Figure 3 shows, topical application of the sunscreen formulations SPF 8 or SPF 15 containing OMC and Parsol® 1789 decreases the fluorescence intensity in the cytoplasm of the stratum spinosum keratinocytes. This indicates that the number of ROS generated within the keratinocytes decreases due to the application of the sunscreen to the skin's surface. The images are representative of those acquired for the strata granulosum and basale as well. Table II lists the % reduction_{avg} in the fluorescence signal detected for each viable epidermal stratum of both the breast and facial skin samples tested.

It is both interesting and important to compare the data acquired from the two different individuals (Table II). The sunscreen combination tested attenuates UVB by approximately 80% for SPF 8 and 90% for SPF 15. Thus, we would expect that the amount of ROS detected in the layers below the skin's surface, where the sunscreen remains, would be 10% less for samples to which have been applied SPF 15 vs SPF 8 sunscreen. In fact, this is what is detected in the breast tissue studied. SPF 8 sunscreen reduces the amount of ROS generated by 84.7%; increasing the SPF to 15 improves the reduction of ROS to 90.1%. These values are consistent with the absorptive properties of the sunscreens used. However, in contrast, the application of SPF 8 and SPF 15 sunscreens to the facial samples yields 42% and 79% reductions in ROS levels, respectively. This correlates to an almost 40% decrease in the number of ROS that are generated in skin to which has been applied the SPF 15 rather than the SPF 8 sunscreen, which is not consistent with

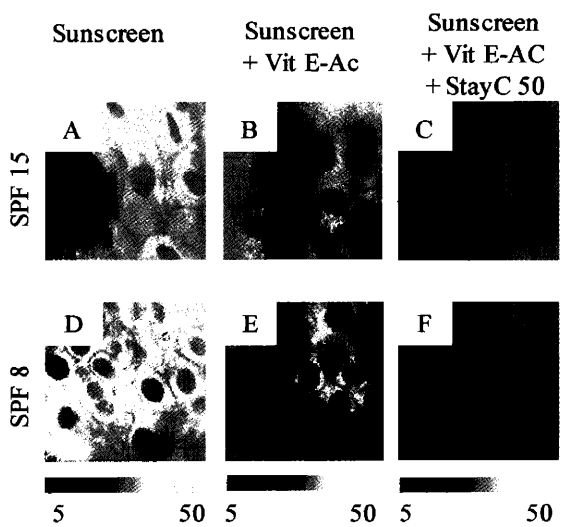

Figure 3. Two-photon fluorescence intensity images of the stratum spinosum of human *ex vivo* breast skin following irradiation by 1600 J m^{-2} UV. Displayed are images of skin with SPF 15 (A–C) and SPF 8 (D–F) OMC and Parsol® 1789 sunscreen (A,D), the sunscreen plus vitamin E acetate (B,E), and the sunscreen plus vitamin E acetate and sodium ascorbyl phosphate (STAY-C® 50) applied topically to the skin's surface (C,F). Image 3C is predominantly blue in color, indicating an almost complete absence of ROS. Note the absence of apparent cell structure due to the lack of fluorescence and thus detectable ROS.

Table II
Comparison of % Reduction$_{avg}$ in R123 Fluorescence (i.e., ROS level) in the Viable Layers of Human Skin Following Application of SPF 8 or SPF 15 OMC +Parsol 1789 Sunscreen and Antioxidants

	% Reduction$_{avg}$ (± standard deviation)			
	Breast		Facial	
	SPF 8	SPF 15	SPF 8	SPF 15
+OMC, Parsol® 1789	84.7 (1.1)	90.1 (1.1)	42.2 (4.2)	79.4 (2.0)
+OMC, Parsol® 1789, vitamin E acetate	88.3 (0.8)	91.9 (0.9)	41.8 (6.5)	79.0 (4.2)
+OMC, Parsol® 1789, vitamin E acetate, STAY-C® 50	91.7 (1.1)	95.5 (0.5)	54.0 (2.4)	84.1 (3.7)

the absorptive property difference of ~10% between the two formulations. This dramatic change is not attributed to differences between skin samples. Cellular, pigmentation, and structural differences that may contribute to variability in the level of ROS detected *between* skin samples would not affect results obtained from the *same* skin sample to which the different SPF formulations have been applied. The % reduction$_{avg}$ values may differ between individual skin samples due to differences in the application of the sunscreen formulations. Although the FDA-approved amount (2 mg cm^{-2}) of sunscreen formulation was first measured prior to application, it is possible that less adhered to the facial skin as opposed to the breast skin. As a result, the total amount of formulation applied may be inconsistent between individual samples. Thus, UV attenuation by the sunscreens on each skin sample may differ. The data are consistent with the conclusion that the amount of sunscreen present upon the skin determines the amount of UV light that penetrates through the stratum corneum, which will in turn affect the amount of ROS that are generated in the cells below the stratum corneum. Specifically, the more sunscreen present at the skin's surface, the less UV light reaches the nucleated keratinocytes and the fewer ROS generated. The data indicate that sunscreens provide incomplete protection against ROS generation.

As Figure 3 shows, however, improved ROS photoprotection is achieved with the addition of the bioconvertible antioxidants vitamin E acetate and STAY-C® 50. The addition of vitamin E acetate either to the SPF 8 or SPF 15 formulation reduces the amount of ROS generated within the viable epidermis. The decrease in ROS production can be seen directly by comparing the fluorescence intensity images Figures 3A against 3B and Figure 3D against Figure 3E, which indicate that vitamin E acetate reduces the amount of ROS generated in the lower viable epidermis. We can calculate the % decrease in ROS due to the addition of vitamin E acetate using the fluorescence intensity values that correspond to the images in Figure 3. Using the breast tissue data, the average % decrease (for both the SPF 8 and 15 data) between the average of the +vitamin E acetate formulation and the sunscreen-only formulations is 20.9% ± 3.9% (Figure 4).

The addition of both antioxidant precursors yields the best ROS photoprotection. As indicated in Figure 3C by the dominant blue-green colors, the ROS generated are dramatically quenched by the addition of the two antioxidant precursors. In addition, note that almost all ROS are quenched following application of the SPF 15-dual antioxidant formulation. The addition of vitamin C to either the SPF 8 or SPF 15 formulation leads to an average % decrease relative to the sunscreen-only formulations of 50.4% ± 5.2% for the breast tissue (Figure 4).

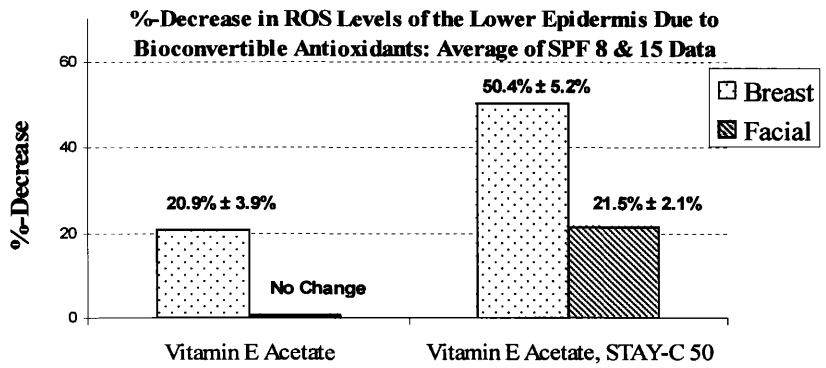

Figure 4. The % decrease in ROS levels, compared to the sunscreen-only formulations, in the lower, viable epidermis due to the addition of antioxidant precursors. All fluorescence intensity data acquired for both skin samples and at both SPF values are used to calculate % decrease. Each bar in the graph represents the average decrease in ROS due to the addition of the antioxidant(s) to the sunscreen formulations.

However, it should be noted that the % decrease in ROS levels in the lower epidermis is less for the facial skin data. As discussed above, this is most likely due to uneven application of the formulation and bioconversion of the antioxidant precursors to active antioxidants.

We attribute the quenching of ROS to the presence of the antioxidants vitamin E and vitamin C generated from the enzymatic conversion of vitamin E acetate and sodium ascorbyl phosphate, respectively. The presence of esterase and phosphatase enzymes in the epidermis naturally converts the photostable antioxidant precursors to their active forms. Enzymatic activity in the studied samples was confirmed using two-photon fluorescence imaging. Figure 5 shows fluorescence intensity images of the stratum granulosum of the *ex vivo* facial skin sample incubated with the enzymatic fluorescence probe calcein-am. In the presence of esterase activity, nonfluorescent calcein-am is converted to fluorescent calcein, which gives rise to the increased fluorescence intensity above that detected from the images either of calcein-am solution or of skin autofluorescence. Similarly, phosphatase activity is confirmed by the presence of fluorescence following the conversion of nonfluorescent FDP to fluorescein (data not shown). Bioconversion of vitamin E acetate and sodium ascorbyl phosphate, and the consequent quenching of UV-induced ROS by vitamin E and vitamin C, are consistent with the enzymatic activity images showing the presence of esterase and phosphatase activity in *ex vivo* human skin. In addition, Trivedi *et al.* (17) report that vitamin E decreases the

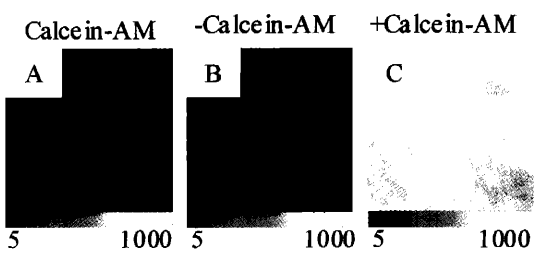

Figure 5. Fluorescence intensity images of (A) the esterase activity probe calcein-am in solution, (B) skin autofluorescence, and (C) the stratum granulosum of calcein-am-incubated *ex vivo* facial skin.

permeability coefficient of skin, which would enhance penetration of the antioxidant precursors, allowing them to penetrate over the three-hour incubation time to the stratum granulosum and lower layers. It has also been determined that bioconversion of vitamin E acetate to its active antioxidant form is enhanced by UV irradiation (18).

It should be noted that *ex vivo* skin may differ from *in vivo* skin in its ROS generating and enzymatic activities. Although media and refrigeration, as used in our experiments, routinely maintain for several days skin grafts for tissue transplants, their ability to prevent any degradation in biochemical processes in the skin is unknown. More or less ROS may be generated *in vivo* than *ex vivo* due to differences in UV chromophore content. Mitochondria are a primary source of ROS in respiring cells naturally and also following UV irradiation (19,20). Although treatment of our *ex vivo* samples does not destroy mitochondrial respiration (1), differences between the *ex vivo* and *in vivo* environments may be great enough to contribute to changes in the amount of ROS detected. Similarly, it is unclear how enzymatic activity is affected by an *ex vivo* environment compared with an *in vivo* environment. Until the recent advent of two-photon microscopy techniques, researchers have not had the tools to acquire data for direct comparison of the biochemistries of *in vivo* and *ex vivo* tissue samples. In addition, with our ever-increasing knowledge of the importance of the photobiological effects of UVA radiation, the use of a UV source that more closely mimics the solar spectrum may prove important when conducting more detailed experiments. We are currently developing methods to translate the method described herein to explore these issues and, for more specific use, to compare ROS generation in human subjects with *ex vivo* skin samples. In addition, we are conducting further studies to compare the effect of antioxidants alone upon ROS generation within the epidermis.

CONCLUSIONS

The addition of the bioconvertible antioxidants vitamin E acetate and sodium ascorbyl phosphate improve sunscreen photoprotection by forming the antioxidants vitamins E and C, respectively, within the epidermis. As a result, an antioxidant reservoir is formed within the epidermis and the ROS that are generated by the residual UV photons, which are not absorbed by sunscreen molecules in the stratum corneum, are quenched. With additional work using two-photon fluorescence microscopy and broad-spectrum solar-simulating light, a detailed study of the effects of any topical formulation upon ROS generation can be accomplished. Because currently available fluorophores that detect ROS are not approved by the FDA for human use, experiments would have to be conducted *in vitro* on either *ex vivo* skin or living skin equivalents, which we have found to be excellent models (1). Other ingredients like nanofine $Ti:O_2$, lipids, and esters may have important effects on ROS levels, which could be determined through this method.

ACKNOWLEDGMENTS

This work was supported by grants from the Skin Cancer Foundation, the Cancer Research Foundation of America, and Roche Vitamins Inc. The Laboratory for Fluorescence Dynamics at the University of Illinois is supported by NIH grant PHS P41-RR03155.

REFERENCES

(1) K. M. Hanson and R. M. Clegg, Observation and quantification of ultraviolet-induced reactive oxygen species generation in *ex vivo* human skin, *PNAS,* **76,** 57–63 (2002).
(2) Q. Chen and B. N. Ames, Senescence-like growth arrest induced by hydrogen peroxide in human diploid fibroblast F65 cells, *PNAS,* **91,** 4130–4134 (1994).
(3) Q. Chen, A. Fischer, J. D. Reagan, L. J. Yan, and B. N. Ames, Oxidative DNA damage and senscence of human diploid fibroblast cells, *PNAS,* **92,** 4337–4341 (1995).
(4) K. M. Hanson, B. Li, and J. D. Simon, A spectroscopic study of the epidermal chromophore trans-urocanic acid, *J. Am. Chem. Soc.,* **119,** 2715–2721 (1997).
(5) K. M. Hanson and J. D. Simon, Epidermal trans-urocanic acid and the UVA-induced photoaging of the skin, *PNAS,* **95,** 10576–10578 (1998).
(6) I. Iwai, M. Hatao, M. Nagnauma, Y. Kumano, and M. Ichihashi, UVA-induced immune suppression through an oxidative pathway, *J. Invest. Dermatol.,* **112,** 19–24 (1999).
(7) M. A. Pathak and M. D. Caronare, in *Biological Responses to Ultraviolet A Radiation,* F. Urbach, Ed. (Valdenmar, Overland Park, KS, 1992), pp. 189–208.
(8) G. F. Vile and R. M. Tyrrell, *Free Rad. Biol. Med.,* **18,** 721–722 (1995).
(9) M. Wlaschek, J. Wenk, P. Brenneisen, K. Briviba, A. Scwarz, H. Sies, and K. Scharfetter-Kochanek, Singlet oxygen is an early intermediate in cytokine-dependent ultraviolet-A induction of interstitial collagenase in human dermal fibroblasts *in vitro, FEBS Lett.,* **413,** 239–242 (1997).
(10) O. W. Health, Intersun: The Global UV Project (United Nations, New York, 1995).
(11) M. Ichihashi, N. U. Ahmed, A. Budiyanto, A. Wu, T. Bito, M. Ueda, and T. Osawa, Preventive effect of antioxidant on ultraviolet-induced skin cancer in mice. *J. Dermatol. Sci., (Suppl. 1),* **23,** S45–S50 (2000).
(12) F. Dreher and H. Maibach, Protective effects of topical antioxidants in humans. *Curr. Probl. Dermatol.,* **29,** 157–164 (2001).
(13) S. R. R. Branch, *Surfrad Network UV Monitoring,* NOAA (2001).
(14) B. R. Masters, P. T. C. So, and E. Gratton, Multiphoton excitation fluorescence microscopy and spectroscopy of *in vivo* human skin, *Biophys. J.,* **72,** 2405–2412 (1997).
(15) R. P. Haughland, *Handbook of Fluorescent Probes and Research Chemicals* (Molecular Probes, Eugene, OR, 1998).
(16) K. M. Hanson, M. J. Behne, N. P. Barry, T. M. Mauro, E. Gratton, and R. M. Clegg, Two-photon fluorescence lifetime imaging microscopy of the skin stratum corneum pH gradient, *Biophys. J.,* **83,** 1682–1690 (2002).
(17) J. S. Trivedi, S. L. Krill, and J. J. Fort, Vitamin E as a human skin penetrating enhancer, *Eur. J. Pharm. Sci.,* **3,** 241–243 (1995).
(18) K. A. Kramer-Strickland and D. C. Liebler, Effect of UVB on hydrolysis of alpha-tocopherol acetate to alpha-tocopherol in mouse skin, *J. Invest. Dermatol.,* **111,** 302–307 (1998).
(19) E. Cadenas and K. J. A. Davies, Mitochondrial free radical generation, oxidative stress, and aging. *Free Rad. Biol. Med.,* **29,** 222–230 (2000).
(20) R. Gniadecki, T. Thorn, J. Vicanova, A. Petersen, and H. C. Wulf, Role of mitochondria in ultraviolet-induced oxidative stress, *J. Cell. Biochem.,* **80,** 215–222 (2000).